

Systematic convergence in the dynamical hybrid approach for complex systems: A numerically exact methodology

Haobin Wang, Michael Thoss,^{a)} and William H. Miller

Department of Chemistry and Kenneth S. Pitzer Center for Theoretical Chemistry, University of California, Berkeley, California 94720-1460 and Chemical Sciences Division, Lawrence Berkeley National Laboratory, Berkeley, California 94720

(Received 28 February 2001; accepted 23 May 2001)

An efficient method, the self-consistent hybrid method, is proposed for accurately simulating time-dependent quantum dynamics in complex systems. The method is based on an iterative convergence procedure for a dynamical hybrid approach. In this approach, the overall system is first partitioned into a “core” and a “reservoir” (an initial guess). The former is treated via an accurate quantum mechanical method, namely, the time-dependent multiconfiguration self-consistent field or multiconfiguration time-dependent Hartree approach, and the latter is treated via a more approximate method, e.g., classical mechanics, semiclassical initial value representations, quantum perturbation theories, etc. Next, the number of “core” degrees of freedom, as well as other variational parameters, is systematically increased to achieve numerical convergence for the overall quantum dynamics. The method is applied to two examples of quantum dissipative dynamics in the condensed phase: the spin-boson problem and the electronic resonance decay in the presence of a vibrational bath. It is demonstrated that the method provides a practical way of obtaining accurate quantum dynamical results for complex systems. © 2001 American Institute of Physics.

[DOI: 10.1063/1.1385561]

I. INTRODUCTION

The treatment of quantum effects in large chemical/biochemical systems is a challenging task in chemical reaction dynamics. Though significant progress has been made over the past few years in the development of rigorous quantum mechanical basis set (in full configuration-interaction context) methods, they are at present limited to relatively small molecular systems in most of the applications. To describe quantum effects in large systems one is thus necessarily interested in developing and applying more approximate methods where the numerical effort scales more favorably with the number of degrees of freedom than the conventional quantum mechanical basis set approaches. Among these, the popular mixed quantum-classical approaches, such as the (partially) classical Ehrenfest model¹⁻⁶ [usually called the time-dependent self-consistent field (TDSCF) model though in this paper we reserve TDSCF for a purely quantum mechanical treatment] and the surface hopping model,⁷⁻¹⁰ are very useful approximations in many situations. The semiclassical initial value representation (SC-IVR) is now also undergoing a rebirth of interest as a practical way of incorporating quantum effects into classical MD simulations.¹¹ Further development of these methods and their applications to interesting problems is an active field of research.

Despite of their usefulness in many situations, it is often difficult to estimate and control the error introduced in these approximations. As a result, one can never be certain of the accuracy achieved in practical applications unless the true

quantum mechanical answer is known. It is thus desirable to develop a method which, at least in principle, can be systematically improved to achieve numerically exact results. Such is the purpose of the present paper.

We begin with an ansatz similar to that in most of the hybrid methods, i.e., the overall molecular system is first partitioned into a “core” and a “reservoir.” The former is treated via an accurate quantum mechanical method, whereas the latter is treated more approximately. Different from the previous hybrid methods, we put such a partitioning into a framework that resembles a common variational calculation. An iterative procedure is carried out to check the convergence of the result by systematically increasing the number of degrees of freedom in the “core,” similar to increasing the number of basis functions (or other variational parameters) in a basis set calculation. We emphasize that different from many previously attempted methods, partitioning the overall system into a “core” and a “reservoir” is unambiguous in our proposed method. The true quantum dynamical result, by definition, should be obtained when all the degrees of freedom are in the “core.” In practice, however, convergence is achieved in many situations well before such a rigorous level, and the method can be regarded as numerically exact. On the other hand, one may also treat the “core” and the “reservoir” by different approximate theories that are appropriate at different physical limits. The approach is thus semi-empirical in nature and may have difficulties at intermediate physical regimes, such that the “core”–“reservoir” partition becomes ambiguous. Such methods are certainly useful in many situations, but are not the subject of the present paper.

Furthermore, we will focus on methods that are local in time, which implies that we shall only consider methods that

^{a)}Author to whom correspondence should be addressed: Theoretische Chemie, Technische Universität München, D-85747 Garching, Germany.

treat all the degrees of freedom explicitly. It should be pointed out that hybrid methods can also be developed using a general master equation-type approach,¹² where a memory kernel is obtained by integrating out some degrees of freedom, e.g., a kernel related to the Feynman–Vernon influence functional¹³ for the harmonic bath. The iterative procedure in this approach, however, involves a high-rank rank tensor and, therefore, further approximations need to be adopted to make the approach practical.¹²

There exist many ways of treating the “core”–“reservoir” at a hybrid level. The essential requirement is that the quantum mechanical method used to treat the “core” should be both accurate (i.e., in principle numerically exact) and efficient, and the approximate method of treating the “reservoir” should be easily implementable with reasonable accuracy. The former ensures that a moderately large number of “core” degrees of freedom (e.g., the size of a common organic molecule) can be treated in a numerically exact fashion, so that the converged result is approached in the full “core” limit, whereas the latter ensures both numerical efficiency and the attainment of certain physical limits. Due to interactions between the “core” and the “reservoir,” the equations of motion for the two parts are dynamically coupled through a self-consistent procedure.

A candidate for treating the “core” is thus a basis set method for solving the time-dependent Schrödinger equation. Specifically, we choose to use a time-dependent multi-configuration self-consistent field (TD-MCSCF) approach. For situations where Bose–Einstein statistics is applied, it is the multiconfiguration time-dependent Hartree (MCTDH) approach developed by Meyer and co-workers^{14,15} (which allows one to treat a rather large boson-system quantum mechanically^{16,17}). Otherwise (e.g., for multiparticle electronic systems) use of the Slater determinant may be necessary. In a previous paper,¹⁸ it was demonstrated that this approach can be used to solve the generic model for electron transfer reactions in the condensed phase, the spin-boson problem, as efficiently as the usual path integral method. The purpose of the present work is to combine it with other approximate methods to further improve its efficiency without loss of accuracy.

Various approximate methods can be used to treat the “reservoir,” e.g., classical mechanics, semiclassical initial value representations, quantum perturbation theories, or other methods.¹⁷ It is usually easy to choose among these methods by examining the physical regimes of the “reservoir.” For example, if the “reservoir” has a rather low characteristic frequency, classical mechanics is often adequate to describe its dynamics for not too low temperatures. On the other hand, if the “reservoir” has a rather high characteristic frequency, one may use some perturbative quantum mechanical methods to describe its impact on the “core.” We emphasize that the choice of these approximate methods, together with the partitioning of the “core” and the “reservoir,” merely serves as a trial “initial guess” for solving the problem. The next step of the method is to systematically include more degrees of freedom in the “core” for the rigorous treatment, a regular convergence test. Similar to situations in many other self-consistent variational methods, the better the

initial guess, the more easily the convergence is achieved.

For practical purpose, we mainly use classical mechanics, with a semiclassical prescription of initial phase space distributions, to treat the “reservoir.” In this case, our self-consistent hybrid method reduces to the conventional mixed quantum-classical model (i.e., classical Ehrenfest) if the “core”–“reservoir” partition is fixed. However, the fact that we do not pre-assume any “quantum” or “classical” part, but rather leave this (often rather arbitrary) division to an iterative convergence procedure, makes the method variational in nature. After an initial guess is made for the “core”–“reservoir” separation, a hybrid quantum-classical dynamical calculation is performed. The result obtained for this particular choice often deviates, to some extent, from the true quantum mechanical answer. Iterations are then carried out by moving some of the “reservoir” degrees of freedom to the “core,” until convergence is achieved.

Usually, the “core” contains the faster degrees of freedom. This is because that these degrees of freedom often exhibit strong quantum mechanical character and also easily treated by a basis set method. The slow modes, on the other hand, can often be described quite well by classical mechanics and, ironically, are very difficult to treat by a basis set method.¹⁹ However, as will be shown in this paper, the distinction between “fast” and “slow” is only a relative measure, which strongly depends on specific problems. Sometimes a “slow reservoir” degree of freedom has to be included in the “fast core” if the physical parameters (e.g., temperature, energy, interaction, etc.) are changed. Other types of partitioning, or approximate methods other than classical mechanics, may be more preferable. These differences only affect the numerical efficiency, since in all situations one needs to perform convergence tests to ensure that the true quantum answer is obtained.

The remaining part of the paper is organized as follows: Section II presents the essential features of our approach. Section III applies the method to the spin-boson problem, and Sec. IV applies it to the electronic resonance decay in the condensed phase. Section V summarizes and concludes.

II. SUMMARY OF THEORY

Consider a general time correlation function for a system–bath-type problem where the interaction between them is switched on at $t=0$ (hereafter $\hbar=1$),

$$C_{AB}(t) = \frac{1}{Q_b} \text{tr}[\hat{\rho}_b \hat{A} e^{i\hat{H}t} \hat{B} e^{-i\hat{H}t}], \quad (2.1a)$$

where \hat{A} and \hat{B} are operators involving the “system” degrees of freedom corresponding to some physical quantities (e.g., the reduced density matrix, dipole moment, etc.), $\hat{\rho}_b$ is the density matrix operator for the “bath” degrees of freedom, and Q_b is its partition function,

$$Q_b = \text{tr}[\hat{\rho}_b]. \quad (2.1b)$$

To evaluate the trace we use a direct product basis $|n\rangle|j\rangle$, where the “bath” states $\{|n\rangle\}$ are the eigenstates of $\hat{\rho}_b$, i.e.,

$$\hat{\rho}_b = \sum_n p_n |n\rangle\langle n|, \quad (2.2a)$$

and the “system” states $\{|j\rangle\}$ are any convenient basis, in which operator \hat{A} has the representation

$$\hat{A} = \sum_j \sum_i a_{ij} |i\rangle \langle j|, \quad (2.2b)$$

where $a_{ij} \equiv \langle i | \hat{A} | j \rangle$. Using this basis to evaluate the trace leads to the following expression for $C_{AB}(t)$:

$$\begin{aligned} C_{AB}(t) &= \frac{1}{Q_b} \sum_n p_n \sum_j \sum_i a_{ij} \langle n | \langle j | e^{i\hat{H}t} \hat{B} e^{-i\hat{H}t} | i \rangle | n \rangle \\ &= \frac{1}{Q_b} \sum_n p_n \sum_j \sum_i a_{ij} \langle \Psi_n^j(t) | \hat{B} | \Psi_n^i(t) \rangle, \end{aligned} \quad (2.3)$$

where

$$|\Psi_n^i(t)\rangle = e^{-i\hat{H}t} |\Psi_n^i(0)\rangle = e^{-i\hat{H}t} |i\rangle |n\rangle. \quad (2.4)$$

Thus, the major computational task is to solve the time-dependent Schrödinger equations

$$i \frac{\partial}{\partial t} |\Psi_n^i(t)\rangle = \hat{H} |\Psi_n^i(t)\rangle, \quad n, i = 1, 2, \dots \quad (2.5a)$$

with initial conditions

$$|\Psi_n^i(0)\rangle = |n\rangle |i\rangle. \quad (2.5b)$$

For a complex molecular system, the rigorous treatment of all degrees of freedom is unfeasible and often unnecessary. One useful approximation, as is commonly made in a hybrid model (such as mixed quantum-classical model), is to partition the overall system into a “core” and a “reservoir.” The former is treated rigorously and the latter more approximately. The total Hamiltonian can be written as

$$\hat{H} = H_{\text{co}}(\hat{\mathbf{p}}_s, \hat{\mathbf{s}}) + H_{\text{rv}}(\hat{\mathbf{p}}, \hat{\mathbf{q}}) + H_I(\hat{\mathbf{p}}_s, \hat{\mathbf{s}}; \hat{\mathbf{p}}, \hat{\mathbf{q}}), \quad (2.6)$$

where $H_{\text{co}}(\hat{\mathbf{p}}_s, \hat{\mathbf{s}})$ and $H_{\text{rv}}(\hat{\mathbf{p}}, \hat{\mathbf{q}})$ represent the uncoupled Hamiltonian for the “core” and the “reservoir,” respectively, and $H_I(\hat{\mathbf{s}}, \hat{\mathbf{p}}_s; \hat{\mathbf{p}}, \hat{\mathbf{q}})$ represent their interactions. The phase space variables $(\mathbf{p}_s, \mathbf{s})$ and (\mathbf{p}, \mathbf{q}) belong to the “core” and the “reservoir,” respectively. The time evolutions of the “core” and the “reservoir” are generally coupled in a self-consistent way.

In our application, the “core” is treated accurately by the time-dependent multiconfiguration self-consistent field (TD-MCSCF) or multiconfiguration time-dependent Hartree (MCTDH) (Ref. 14) approach, which shows promises for dealing with large systems. The approximate method for the “reservoir” can be any convenience choice, so long as it is easily implementable. In many situations, classical mechanics is a reasonable choice. The procedure is thus the usual (partially classical) Ehrenfest model,⁴ with the effective interactions given as

$$\hat{H}_{I,\text{co}}^{\text{eff}}(t) = H_I[\hat{\mathbf{p}}_s, \hat{\mathbf{s}}; \mathbf{p}_t, \mathbf{q}_t], \quad (2.7a)$$

$$H_{I,\text{rv}}^{\text{eff}}(t) = \langle \psi_{\text{co}}(t) | H_I(\hat{\mathbf{p}}_s, \hat{\mathbf{s}}; \mathbf{p}_t, \mathbf{q}_t) | \psi_{\text{co}}(t) \rangle, \quad (2.7b)$$

where $|\psi_{\text{co}}(t)\rangle$ represents the wave function for the “core,” and the Heisenberg operators $(\hat{\mathbf{p}}, \hat{\mathbf{q}})$ for the “reservoir” are replaced by their corresponding (time-dependent) classical

phase space variables $(\mathbf{p}_t, \mathbf{q}_t)$. The dynamics of both the “core” and the “reservoir” are governed by the time-dependent Hamiltonian,

$$\hat{H}_{\text{co}}^{\text{eff}}(t) = H_{\text{co}}(\hat{\mathbf{p}}_s, \hat{\mathbf{s}}) + \hat{H}_{I,\text{co}}^{\text{eff}}(t), \quad (2.8a)$$

$$H_{\text{rv}}^{\text{eff}}(t) = H_{\text{rv}}(\mathbf{p}_t, \mathbf{q}_t) + H_{I,\text{rv}}^{\text{eff}}(t), \quad (2.8b)$$

and the quantum mechanical trace expression in Eq. (2.1a) is also modified as

$$C_{AB}(t) = \frac{1}{Q_b} \int d\mathbf{p}_0 \int d\mathbf{q}_0 \rho_b^{\text{rv}}(\mathbf{p}_0, \mathbf{q}_0) \text{tr}[\hat{\rho}_b^{\text{co}} \hat{A} e^{i\hat{H}t} \hat{B} e^{-i\hat{H}t}], \quad (2.9)$$

where the trace is only over the “core.” The initial density matrix $\hat{\rho}_b$ is split into a “core” part, $\hat{\rho}_b^{\text{co}}$, and a corresponding classical distribution ρ_b^{rv} for the “reservoir.” (Hereby, it is implicitly assumed that the “core” comprises at least all degrees of freedom of the system.) In accordance with the classical treatment of the dynamics of the “reservoir” (based on a semiclassical prescription²⁰), the initial phase space distribution $\rho_b^{\text{rv}}(\mathbf{p}_0, \mathbf{q}_0)$ is obtained by taking the Wigner transform of the corresponding operator $\hat{\rho}_b^{\text{rv}}$,

$$\begin{aligned} \rho_b^{\text{rv}}(\mathbf{p}_0, \mathbf{q}_0) &= \frac{1}{(2\pi)^{N_r}} \int d\Delta \mathbf{q} e^{-i\mathbf{p}_0 \cdot \Delta \mathbf{q}} \\ &\times \left\langle \mathbf{q}_0 + \frac{\Delta \mathbf{q}}{2} \left| \hat{\rho}_b^{\text{rv}} \right| \mathbf{q}_0 - \frac{\Delta \mathbf{q}}{2} \right\rangle, \end{aligned} \quad (2.10)$$

where N_r is the number of “reservoir” degrees of freedom.

The classical Ehrenfest model¹⁻⁶ is chosen for convenience. One may also use a stochastic approach such as the surface hopping model.⁷⁻¹⁰ Both models have their applicable regimes and also certain limitations. Such limitations arise from the approximate classical treatment of the “reservoir” and in general cannot be improved once the “core”–“reservoir” separation is predetermined. One must therefore either use a more accurate method to treat the “reservoir” or move some “reservoir” degrees of freedom to the “core” for accurate treatment. In this paper we take the latter approach.

Thus different from previous applications of a hybrid method, we treat the partition of “core”–“reservoir” as a convergence parameter. In the first step, an initial guess is made for the partition. The dynamical calculation is performed for this particular choice, using the hybrid method such as the Ehrenfest model outlined above. The second step is to move some degrees of freedom from the “reservoir” to the “core,” according to some systematic criteria, and perform the dynamical calculation again for the same physical parameters. This step is repeated by increasing the size of the “core” until numerical convergence is achieved. Since the basis set method used to treat the “core” is in principle numerically exact, this convergence is unambiguous and can be regarded as the true quantum mechanical result.

As has already been mentioned above, within the hybrid approach the choice of the dynamical method for “core” and “reservoir” is not restricted to the mixed quantum-classical approach. At low temperatures and/or fast timescales for the overall system, a mixed quantum-classical model is not efficient since most degrees of freedom need a quantum me-

chanical treatment. In this situation, it is more effective to choose an approximation that bears some quantum mechanical character. For example, a Born–Oppenheimer-type approximation can be made, where the *slower* degrees of freedom are included in the “core” for an accurate treatment, and the faster “reservoir” is treated by quantum perturbation theory. Below, we briefly discuss some details of the implementation for the system–bath problem.

A. The multiconfiguration time-dependent Hartree method

In order to treat a large “core,” we apply the multiconfiguration time-dependent Hartree (MCTDH) method,^{14–16} where the wave function is expanded in time-dependent Hartree products (for Bose–Einstein statistics),

$$|\Psi(t)\rangle = \sum_J A_J(t) |\Phi_J(t)\rangle$$

$$= \sum_{J_1} \sum_{J_2} \cdots \sum_{J_N} A_{J_1 J_2 \cdots J_N}(t) \prod_{k=1}^M |\phi_{J_k}^k(t)\rangle, \quad (2.11a)$$

$$|\Phi_J(t)\rangle = \prod_{k=1}^M |\phi_{J_k}^k(t)\rangle = \prod_{k=1}^M |\phi_{J_k}^k(t)\rangle. \quad (2.11b)$$

$|\phi_{J_k}^k(t)\rangle$ is the “single-particle” (SP) function for the k th SP degree of freedom and M is the number of SP degrees of freedom. Each SP usually contains several (Cartesian) degrees of freedom in our calculation, and for convenience the SP functions within the same SP degree freedom are chosen to be orthonormal.

The working equations within MCTDH scheme are¹⁴

$$i\dot{A}_J(t) = \langle \Phi_J(t) | \hat{H}_c | \Psi(t) \rangle$$

$$= \sum_L \langle \Phi_J(t) | \hat{H}_c | \Phi_L(t) \rangle A_L(t), \quad (2.12a)$$

$$i|\dot{\phi}^k(t)\rangle = \hat{h}_k |\phi^k(t)\rangle + (1 - \hat{P}^k) (\hat{\rho}^k)^{-1} \langle \hat{H}_c(t) | \phi^k(t) \rangle |\phi^k(t)\rangle, \quad (2.12b)$$

$$\hat{H} = \hat{H}_c + \sum_k \hat{h}_k. \quad (2.12c)$$

Here \hat{h}_k is an arbitrary Hermitian operator that only affects the numerical efficiency, $|\phi^k(t)\rangle = \{|\phi_1^k(t)\rangle, |\phi_2^k(t)\rangle, \dots\}^T$ denotes the symbolic column vector of SP functions for the k th SP degree of freedom, \hat{P}^k is the SP space projection operator,

$$\hat{P}^k(t) = \sum_n |\phi_n^k(t)\rangle \langle \phi_n^k(t)|, \quad (2.13)$$

$\langle \hat{H}_c(t) \rangle^k$ is the mean-field operator acting only on the k th SP,

$$\langle \hat{H}_c(t) \rangle_{nm}^k = \langle G_n^k(t) | \hat{H}_c | G_m^k(t) \rangle, \quad (2.14)$$

and $(\hat{\rho}^k)^{-1}$ is the pseudo-inverse of the reduced density matrix,

$$\hat{\rho}_{nm}^k(t) = \langle G_n^k(t) | G_m^k(t) \rangle, \quad (2.15)$$

where $|G_n^k\rangle$, the “single-hole” function, is defined as

$$|G_n^k\rangle = \sum_{j_1} \cdots \sum_{j_{k-1}} \sum_{j_{k+1}} \cdots \sum_{j_M} A_{j_1 \cdots j_{k-1} n j_{k+1} \cdots j_M} \times |\phi_{j_1}^1\rangle \cdots |\phi_{j_{k-1}}^{k-1}\rangle |\phi_{j_{k+1}}^{k+1}\rangle \cdots |\phi_{j_M}^M\rangle, \quad (2.16a)$$

so that

$$|\Psi\rangle = \sum_n |\phi_n^k\rangle |G_n^k\rangle. \quad (2.16b)$$

Finally, each SP function is expanded in a chosen (time-independent) basis set $\{|\varphi_i^k\rangle\}$,

$$|\phi_n^k(t)\rangle = \sum_i c_{i,n}^k(t) |\varphi_i^k\rangle. \quad (2.17)$$

B. Basis sets and single-particle functions

The primitive basis functions can be any convenient choice. For example, for the spin-boson problem the two diabatic states are used as basis for the electronic degree of freedom, and the harmonic oscillator wave functions are used as basis for the bath. Several degrees of freedom are then combined together to form one SP. The number of primitive basis functions/states within one SP consists of all possible combinations of the basis functions for each degree of freedom, and may be a very large number. These primitive basis functions, $|\varphi_i^k\rangle$, are then contracted using an adiabatic reduction technique,²¹ where states with energies higher than E_{cut} are rejected with E_{cut} a convergence parameter. Such a contraction can be very aggressive (several orders of magnitude of reduction in number of basis functions) without losing accuracy, as demonstrated in many applications, and is essential for practical applications of MCTDH to a large number of (e.g., ~ 100) degrees of freedom.

For simplicity, the number of SP functions for each SP degree of freedom is chosen to be the same. We find that usually three SP functions for each SP degree of freedom gives satisfactory results. Thus unless specified otherwise, this number is used for most of the examples in this paper (though occasionally more are needed). This number is rather insensitive to the specific way of combining several degrees of freedom into one SP, as found in our applications. This is certainly problem-dependent and convergence needs to be checked for every case.

C. Monte Carlo procedure for trace evaluation

If all degrees of freedom are included in the “core” and treated quantum mechanically, then the trace expression in Eq. (2.3) involves the total number of initial wave functions for the real time propagation. A direct summation is possible if the initial density matrix contains only a few pure states, e.g., very low temperature or a specific preparation of the initial wave packet. At high temperatures, there are many states that contribute to the correlation function in Eq. (2.1a), and inclusion of all such states is numerically unfeasible. Situations are similar for the mixed quantum-classical case, Eq. (2.9), where quadrature summations are not feasible for the classical phase space variables in many dimensions. Thus

we cast the overall integration/trace summation into a Monte Carlo procedure. Both the classical phase space variables $(\mathbf{p}_0, \mathbf{q}_0)$ for the “reservoir” and the quantum states $\{\mathbf{n}\}$ for the “core” are randomly sampled via importance sampling procedure, according to the distribution functions $\rho_b^{\text{rv}}(\mathbf{p}_0, \mathbf{q}_0)$ and $\hat{\rho}_b^{\text{co}}(\mathbf{n})$, respectively.

It is important to note that in the above procedure one does not average over the time-dependent wave functions or quantities related to the single time propagator $e^{-i\hat{H}t}$, which is known to be plagued by the “sign problem.” Instead, physical observables that relate to the Heisenberg operator $e^{i\hat{H}t}\hat{B}e^{-i\hat{H}t}$ are averaged. The procedure is thus very similar to a classical Monte Carlo calculation that is free from the phase oscillations, which is usually converged for a statistical sampling size of 10^2 – 10^4 .

III. THE SPIN-BOSON PROBLEM

In this section, we apply the self-consistent hybrid approach outlined above to the spin-boson model with the popular Ohmic spectral density. The focus of the presentation is primarily on the performance of the hybrid approach and its convergence properties with respect to the various parameters. A few comparisons are also made with some approximate methods in order to demonstrate the necessity of carrying out numerically exact simulations for certain physical regimes. More thorough discussions of the physics of the spin-boson system as a model of electron-transfer reactions in a solvent, as well as comparisons with a variety of approximate approaches, are given in the following paper.²²

A. Background of the problem

The spin-boson model is a generic model for electron transfer reactions in the condensed phase,^{23,24} where two discrete (electronic) states, corresponding to the donor and acceptor states in electron transfer processes, are linearly coupled to a phonon bath. In the diabatic representation, the Hamiltonian is

$$\hat{H} = \hat{H}_B + (|1\rangle\langle 1| - |2\rangle\langle 2|)\hat{H}_c + \epsilon(|1\rangle\langle 1| - |2\rangle\langle 2|) + \Delta(|1\rangle\langle 2| + |2\rangle\langle 1|), \quad (3.1)$$

where the bath Hamiltonian H_B and the system–bath coupling H_c are expressed in the mass-weighted coordinate system as

$$H_B = \sum_j \frac{1}{2}(P_j^2 + \omega_j^2 Q_j^2), \quad (3.2a)$$

$$H_c = \sum_j c_j Q_j. \quad (3.2b)$$

The central property of the bath is its spectral density,²³

$$J(\omega) = \frac{\pi}{2} \sum_j \frac{c_j^2}{\omega_j} \delta(\omega - \omega_j), \quad (3.3)$$

which characterizes the effect of the bath on transitions between the electronic states. In this paper we choose it in the popular Ohmic form with an exponential cutoff,

$$J_o(\omega) = \frac{\pi}{2} \alpha \omega e^{-\omega/\omega_c}, \quad (3.4)$$

which has been extensively studied via various approximate approaches and also accurate numerical path integral methods, and is thus ideal for comparison purposes.

The observable of interest is the time-dependent population difference of the two electronic states, $\sigma_z(t)$,

$$\sigma_z(t) = \frac{1}{Q_B} \text{tr}[e^{-\beta\hat{H}_B}|1\rangle\langle 1|e^{i\hat{H}t}\hat{\sigma}_ze^{-i\hat{H}t}], \quad (3.5a)$$

$$\hat{\sigma}_z = |1\rangle\langle 1| - |2\rangle\langle 2|, \quad (3.5b)$$

where the initial density matrix is chosen to be factorized, with the initial electronic state set to state $|1\rangle$ and a thermal distribution for the phonon bath.

The continuous bath spectral density of Eq. (3.4) can be discretized to the form of Eq. (3.3) via the relation,

$$c_j^2 = \frac{2}{\pi} \omega_j \frac{J_o(\omega_j)}{\rho(\omega_j)}, \quad (3.6a)$$

where $\rho(\omega)$ is a density of frequencies satisfying

$$\int_0^{\omega_j} d\omega \rho(\omega) = j, \quad j = 1, \dots, N_b. \quad (3.6b)$$

The precise functional form of $\rho(\omega)$ does not affect the final answer if enough bath modes are included, but it does affect the efficiency of solving the problem (i.e., the number of bath modes needed to represent the continuum). Here we choose $\rho(\omega)$ to accurately reproduce the reorganization energy with any number of bath modes, i.e.,

$$\rho(\omega) = \frac{N_b}{\omega_c} \frac{e^{-\omega/\omega_c}}{1 - e^{-\omega_m/\omega_c}}, \quad (3.7)$$

where ω_m is the largest frequency of the bath modes considered in the calculation, which is chosen as $\omega_m = 5 - 10\omega_c$.

The expression for $\sigma_z(t)$ is thus in the form of Eq. (2.3), which can be solved by the hybrid method described above. Different from a molecular system with a fixed number of degrees of freedom, convergence tests needs to be performed to ensure that the number of discrete phonon modes is sufficient to represent the condensed phase environment. For the examples studied in this paper, this number ranges from 30 to 400.

B. Results and discussion

The methodology presented in the previous sections is in principle (numerically) exact, as long as one chooses enough variational parameters. This includes choosing a sufficient number of bath modes to represent the continuum, including enough number of degrees of freedom in the “core” for accurate quantum mechanical treatment, as well as other parameters. Calculations have been performed for parameter regimes where numerical path integral results are available, e.g., those reported in Refs. 25 and 26, with which our converged results are all in quantitative agreement. Below we discuss our results and their convergence properties with respect to other regimes.

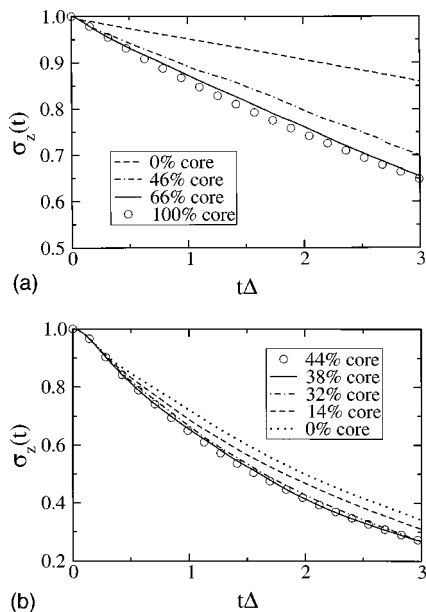


FIG. 1. Convergence of $\sigma_z(t)$ with respect to the percentage of the bath modes (starting from the high frequency end of the spectral density) in the “core.” (a) $\epsilon=0, \omega_c/\Delta=40, \alpha=0.5, \beta\Delta=0.25$; (b) $\epsilon=0, \omega_c/\Delta=10, \alpha=0.5, \beta\Delta=0.25$.

As was discussed in Sec. II, within the hybrid approach different approximate methods can be used to treat the dynamics of the “reservoir.” Furthermore, depending on the particular situation under consideration, the strategy for the “initial guess” of the “core”–“reservoir” partition may be different. For most of the numerical results presented below we have used the mixed quantum-classical approach and a partitioning where the two electronic states are always included in the “core.” The number of bath modes in the “core” is then systematically increased from the high-frequency end of the spectral density. However, as will be shown in the following paragraphs and various figure captions, in some cases other criteria in selecting the “core” degrees of freedom may be preferable (in terms of numerical efficiency). In particular, we have found that for situations of very low temperature hybrid methods other than mixed quantum-classical are more efficient. Since the method is self-consistent, the “correct” “core”–“reservoir” partition for a specific parameter regime is iteratively found from convergence tests, and depends on the physical parameters such as temperature, electron–phonon coupling, etc.

Figure 1 shows the convergence of $\sigma_z(t)$ with respect to the percentage of the bath modes in the “core.” (A discretization of the bath with a total of 50 vibrational modes provides converged results for the parameter regime considered here.) The parameters in Fig. 1(a) corresponds to a rather high bath characteristic frequency, $\omega_c/\Delta=40$, and a relatively low temperature, $\beta\omega_c=10$, for the bath. It is thus expected that a relatively high percentage of the bath modes have to be treated quantum mechanically. This is indeed what we have found. It is seen that when no phonon modes are included in the “core” (i.e., classical Ehrenfest model for the spin-boson problem²⁷), the population decay is much slower than the true quantum mechanical result displayed as

hollow circles. Results are systematically improved as more bath modes are included in the “core.” Within the statistical error, the results are essentially converged with roughly 70% modes included in the “core.”

As the percentage of the bath modes in the “core” increases, the variational parameters in the MCTDH treatment of the “core” may not remain the same. In the above example, three SP functions per each SP degree of freedom gives converged MCTDH result for cases where less than 70% modes are treated in the “core.” This number is not sensitive to the specific ways of grouping several bath modes into the SP degrees of freedom. However, for higher percentage of the “core” bath modes, the minimum number of SP functions per SP degree of freedom increases to five, again rather insensitive to the particular grouping of modes. This suggests that for low-frequency modes the orbitals are split into many nodes and more SP functions are required to describe their reduced density matrices. It is inappropriate to describe the overall dynamics with a single Hartree approximation for these low frequency modes (which is a popular assertion). Instead, one has to use even *more* SP functions. This is related to the fact that the classical limit (decoherent but with many configurations) is different from the single Hartree limit.

Figure 1(b) illustrates the convergence property of $\sigma_z(t)$ for a slower bath, $\omega_c/\Delta=10$, where other parameters are kept the same as in Fig. 1(a). It is natural to expect that a higher percentage of the modes can be treated classically than that in Fig. 1(a), which is confirmed by the results shown in the figure. Approximately 40% of the (higher frequency) “core” modes gives converged population decay, although the usual classical Ehrenfest model (0% bath modes in the “core”) already gives reasonable answers in this case. As the bath characteristic frequency ω_c decreases, fewer bath modes need to be included in the “core” for accurate quantum mechanical treatment and classical Ehrenfest model becomes more accurate.

It is interesting to note that in Fig. 1, the Kondo parameter α was chosen to be $\alpha=\frac{1}{2}$, which has been paid special attention in previous literature.²³ In the limit $\omega_c\rightarrow\infty$ and $\beta\omega_c\rightarrow\infty$, a simple expression for $\sigma_z(t)$ is given as [cf., for example, Eq. (5.23) in Ref. 23, note there is a factor of 2 difference in the convention of Δ between Ref. 23 and the current paper]

$$\sigma_z(t) = \exp\left[-2\pi\frac{\Delta^2}{\omega_c}t\right]. \quad (3.8)$$

This can also be viewed as a special limit for the noninteracting-blip approximation (NIBA) (Ref. 23) for sufficiently low temperatures. The parameters in Fig. 1, though satisfying the usual perturbation theory requirement for nonadiabatic electronic transitions, do not fulfill the requirement for Eq. (3.8). As a result, NIBA gives $\sigma_z(t)$'s that are in very good agreement with our simulation, but showing some difference from Eq. (3.8).

In electron-transfer theory, one of the most important parameters is the classical reorganization energy,

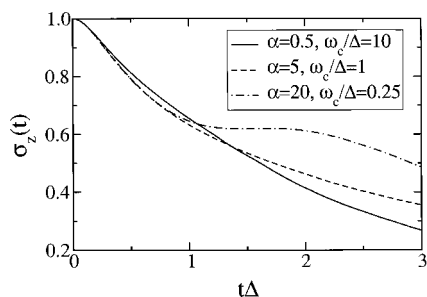


FIG. 2. Dynamics of $\sigma_z(t)$ with respect to different time scales of the bath. The parameters are $\epsilon=0$, $\beta\Delta=0.25$, and the classical reorganization energy $E_r=2\alpha\omega_c=10\Delta$ is set the same for three cases. The percentage of the bath modes (starting from the high frequency end of the spectral density) in the “core” are 38%, 13%, and 0% for $\alpha=0.5$, $\alpha=5$, and $\alpha=20$, respectively; and the number of bath modes are 50, 100, and 200, respectively.

$$E_r = \frac{4}{\pi} \int_0^\infty d\omega \frac{J(\omega)}{\omega}, \quad (3.9)$$

which measures the electron–phonon coupling strength. For Ohmic spectral density in Eq. (3.4), the integral in Eq. (3.9) gives $E_r=2\alpha\omega_c$. Rate constants can be evaluated via the Fermi Golden Rule or NIBA, which gives classical Marcus theory at high temperatures.

This procedure for calculating the rate constant implicitly assumes that there is a sufficient time scale separation between the electronic states and the phonon bath. Caution must be taken in justifying it for realistic systems. As an example, Fig. 2 shows the converged simulations of $\sigma_z(t)$ with respect to different time scales of the phonon bath. It is clear that $\sigma_z(t)$ exhibits an incoherent to coherent transition as the bath becomes slower, despite the fact that $E_r=10\Delta$ is set the same for all cases. So far (to the best of our knowledge), such a transition cannot be predicted by a existing theoretical model.

For incoherent electronic relaxations such as displayed in Figs. 1 and 2, we find that gradually increasing the number of bath modes, starting from the high-frequency end of the spectral density, provides a systematic and efficient way of achieving converged quantum mechanical results. For coherent regimes, however, the electron–phonon couplings are relatively weak and, therefore, some of the high-frequency modes may also be treated classically without losing accuracy in the overall result. This further reduces the percentage of the bath modes which must be included in the “core” and makes the calculation more efficient. Specifically, a characteristic frequency for the electronic states is estimated from its Rabi frequency,

$$\omega_r = 2\sqrt{\epsilon^2 + \Delta^2}. \quad (3.10)$$

The percentage of “core” modes is systematically increased, starting from $\omega = \omega_r$ and moving to both high- and low-frequency ends. The physical implication of this approach is that bath modes with frequencies that are in resonance to the coherent oscillations of electronic populations have major impact to the overall electronic transitions.

Figure 3 illustrates the dynamics of $\sigma_z(t)$ for coherent regimes, where again E_r is fixed and the time scale of the bath is varied. In Fig. 3(a) the electronic bias ϵ is zero, so

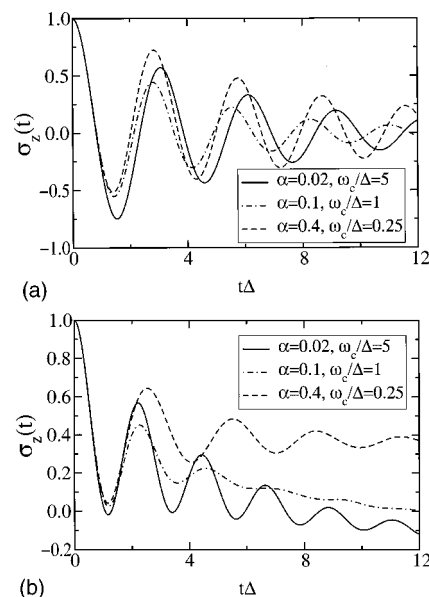


FIG. 3. Dynamics of $\sigma_z(t)$ with respect to different time scales of the bath. The parameters are $\beta\Delta=0.25$, and the classical reorganization energy $E_r=2\alpha\omega_c=0.2\Delta$: (a) $\epsilon=0$. The classical Ehrenfest model (0% bath modes in the “core”) with 50–100 bath modes provides converged results for all three cases. (b) $\epsilon/\Delta=1$. The percentage of the bath modes (centered around $\omega_r=2\sqrt{\epsilon^2+\Delta^2}$) in the “core” are 30%, 24%, and 0% for $\alpha=0.02$, $\alpha=1$, and $\alpha=0.4$, respectively; and the number of bath modes are 50, 50, and 100, respectively.

that $\sigma_z(t) \rightarrow 0$ as $t \rightarrow \infty$, and the change in the bath timescale only affects the oscillation amplitude and period of $\sigma_z(t)$. In Fig. 3(b), the bias is chosen as $\epsilon/\Delta=1$ and the long time limit of $\sigma_z(t)$ is also different as the bath time scale changes.

In a mixed quantum-classical calculation, it is often tempting to separate the overall molecular system into a “fast” and a “slow” part, with the former treated quantum mechanically. This intuitive approach, however, does not work well for situations such as in Fig. 3. The only difference between parameters in Fig. 3(a) and Fig. 3(b) is the electronic energy bias ϵ , and it is seen that it has a major impact on the percentage of modes that need to be treated quantum mechanically. For all three cases in Fig. 3(a) where $\epsilon=0$, the classical Ehrenfest model (0% modes in the “core”) gives converged results. On the other hand, a certain percentage of the bath modes needs to be treated quantum mechanically for a nonzero bias, $\epsilon/\Delta=1$. The most important such modes are those with frequencies close to the Rabi frequency of the electronic states. Calculations have been performed using the same strategy as in Figs. 1 and 2, i.e., gradually increasing the percentage of the “core” modes which start from the high-frequency end of the spectral density, and it is found to be rather inefficient. For example, for the case of $\alpha=0.02$, $\omega_c/\Delta=5$ in Fig. 3(b), more than 70% bath modes need to be put in the “core” to obtain converged results. Among these modes, tests show that those with frequencies much higher than the Rabi frequency, ω_r in Eq. (3.10), can be put to the “reservoir” and treated classically. The resulting “core” thus needs only 30% of the modes to achieve convergence. This suggests that caution must be taken in preassuming a fixed partition of “classical” and

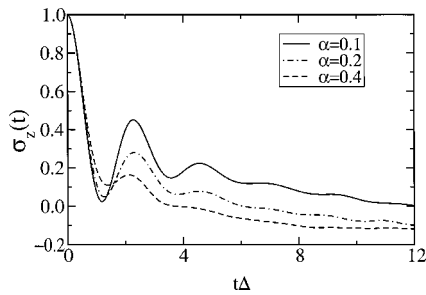


FIG. 4. Dynamics of $\sigma_z(t)$ with respect to different electron–phonon couplings. The parameters are $\epsilon/\Delta=1, \beta\Delta=0.25, \omega_c/\Delta=1$. The percentage of the bath modes (centered around $\omega_r=2\sqrt{\epsilon^2+\Delta^2}$) in the “core” are 24%, 24%, and 30% for $\alpha=0.1$, $\alpha=0.2$, and $\alpha=0.4$, respectively; and the number of bath modes is 70 for all three cases.

“quantum” degrees of freedom. Necessary convergence tests, such as those performed here, need to be carried out to ensure the correct quantum mechanical results. Also, it suggests that physical intuitions that are often used in performing approximate calculations for these regimes need to be rebuilt based on the exact simulations.

In Figs. 1–3, we have shown that the converged percentage of the bath modes in the “core” depends on the temperature, the timescale of the bath, and the electronic energy bias (since the electronic exchange matrix element Δ is used as a basic unit in this paper, it does not serve as a parameter). Figure 4 shows that this percentage may also depend on the electron–phonon coupling, α . The time-dependent population displays a coherent to incoherent transition as the electron–phonon coupling increases, a well known physical phenomenon. However, due to the ill time scale separation between the electron and phonon degrees of freedom, existing analytic theories are not satisfactory in quantitatively describing $\sigma_z(t)$ for large α (e.g., $\alpha=0.4$ in Fig. 4), and neither is the classical Ehrenfest model. In general more “core” modes are needed for convergence to the true quantum result as the electron–phonon coupling increases.

Figures 5 and 6 display dynamics of $\sigma_z(t)$ for a lower temperature, $\beta\Delta=5$. In Fig. 5 the classical reorganization energy E_r is fixed and the characteristic frequency of the bath is varied, whereas in Fig. 6 the dynamics is investigated

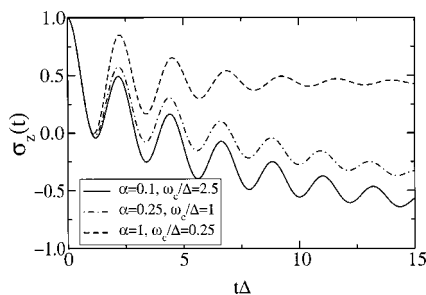


FIG. 5. Dynamics of $\sigma_z(t)$ with respect to different time scales of the bath. The parameters are $\epsilon/\Delta=1, \beta\Delta=5$, and the classical reorganization energy $E_r=2\alpha\omega_c=0.25\Delta$ is set the same for three cases. The percentage of the bath modes (starting from the high frequency end of the spectral density) in the “core” are 80%, 48%, and 20% for $\alpha=0.1$, $\alpha=0.25$, and $\alpha=1$, respectively; and the number of bath modes are 50, 50, and 100, respectively.

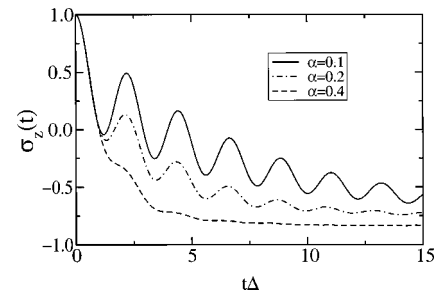


FIG. 6. Dynamics of $\sigma_z(t)$ with respect to different electron–phonon couplings. The parameters are $\epsilon/\Delta=1, \beta\Delta=5, \omega_c/\Delta=2.5$. The percentage of the bath modes (starting from the high frequency end of the spectral density) in the “core” is 80% for all three cases; and the number of bath modes are 50, 50, and 75 for $\alpha=0.1$, $\alpha=0.2$, and $\alpha=0.4$, respectively.

versus the Kondo parameter, α , with other parameters fixed. Due to the lower temperature, more bath modes are needed in the “core” to obtain accurate quantum mechanical results. For simplicity the convergence is shown versus the percentage of the “core” bath modes from the high-frequency end of the spectral density. The same strategy as in Figs. 3 and 4 (i.e., centered around ω_r) can also be used here to reduce the number of “core” bath modes. The savings in computational cost are not as significant, however, because at lower temperature more high-frequency modes need to be treated quantum mechanically. On the other hand, relatively few basis functions are needed for each mode and it is rather easy to perform a MCTDH calculation that includes many modes.

Although the mixed quantum-classical strategy works well for many parameter regimes, it is not efficient for very low temperatures. In this situation almost all the bath modes exhibit strong quantum mechanical character and need to be included in the “core” within a mixed quantum-classical treatment. On the other hand, the hybrid method described above is not restricted to the mixed quantum-classical model. One may choose other approximate methods for treating the “reservoir” that are more efficient at low temperatures, and check convergence in a similar fashion (i.e., by increasing the size of the “core” which is always treated via MCTDH).

As an example, we investigate the dynamics of $\sigma_z(t)$ at very low temperature, where we partition the two electronic states plus the *low-frequency* modes in the “core,” and the *high-frequency* modes in the “reservoir.” A Born–Oppenheimer-type approximation can then be made, where the fast “reservoir” is treated by perturbation theory. It has been shown previously²³ that in this way the high-frequency “reservoir” can be integrated out, resulting in a modified exchange matrix element Δ_{eff} for the slower “core,”

$$\Delta_{\text{eff}} = \Delta \exp \left[\frac{2}{\pi} \int_{\omega_q}^{\infty} d\omega \frac{J(\omega)}{\omega^2} \right]. \quad (3.11)$$

Here ω_q is the “core”–“reservoir” boundary that serves as a convergence parameter. For example, the complete quantum dynamical treatment for the original spin-boson problem is recovered in the $\omega_q \rightarrow \infty$ limit. It should be pointed out that Eq. (3.11) is only valid at nearly zero temperature for the high-frequency “reservoir,” $\beta\omega_q \gg 1$. It is used here for con-

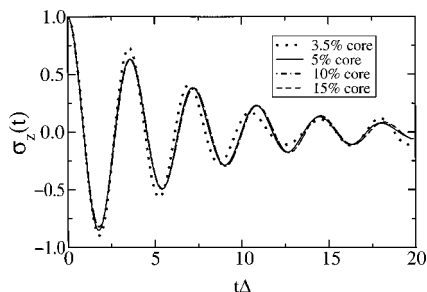


FIG. 7. Convergence of $\sigma_z(t)$ with respect to the percentage of the bath modes (starting from the low frequency end of the spectral density) in the “core.” The parameters are $\epsilon=0, \omega_c/\Delta=60, \alpha=0.05, \beta\Delta=10$, and the number of bath modes is 300.

venience. In general, one can carry out perturbation calculations for each “reservoir” mode explicitly without integrating out them.

Figure 7 illustrates the convergence of $\sigma_z(t)$ versus the percentage of the “core” modes, starting from the low-frequency end of the spectral density. The parameters are $\epsilon=0, \omega_c/\Delta=60, \alpha=0.05, \beta\Delta=10$, which corresponds to a rather low temperature. In order to represent the continuum, 300 bath modes are needed in the discretization. The “core” is treated via the MCTDH method as described above, whereas the effect of the “reservoir” is given by Eq. (3.11). For this particular case, convergence is reached when including 10% bath modes in the “core” for accurate dynamical treatment, although 5% bath modes in the “core” already provides a good description.

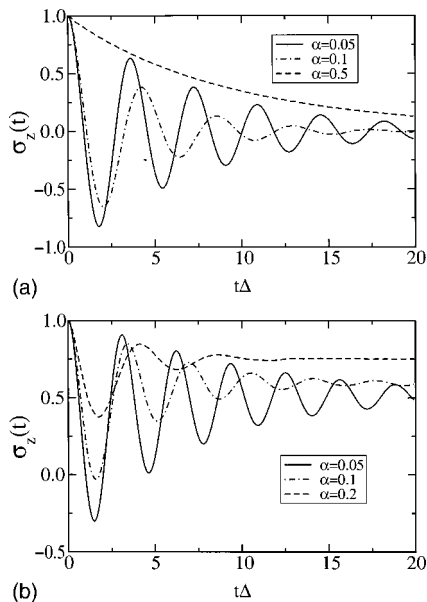


FIG. 8. Dynamics of $\sigma_z(t)$ with respect to different electron–phonon coupling α for $\beta\Delta=10$ and $\omega_c/\Delta=60$: (a) $\epsilon=0$. The percentage of the bath modes (starting from the low frequency end of the spectral density) in the “core” are 10%, 10%, and 15% for $\alpha=0.05, \alpha=0.1$, and $\alpha=0.5$, respectively, and the number of bath modes is 300 for all three cases. For $\alpha=0.5$, five SP functions are used for each SP. (b) $\epsilon/\Delta=-0.5$. The percentage of the bath modes (starting from the low frequency end of the spectral density) in the “core” are 10%, 15%, and 15% for $\alpha=0.05, \alpha=0.1$, and $\alpha=0.2$, respectively; and the number of bath modes are 300, 350, and 400, respectively.

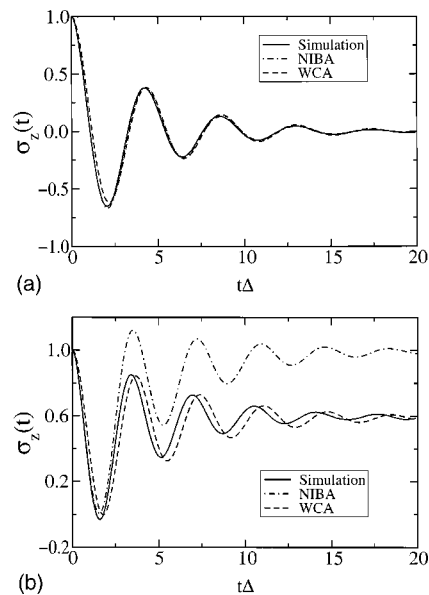


FIG. 9. Comparisons of $\sigma_z(t)$ between converged simulation results, the NIBA, and the weak-coupling approximation (WCA). The parameters are $\alpha=0.1, \beta\Delta=10$, and $\omega_c/\Delta=60$. The number of bath modes is 350, and 15% low-frequency end of the spectral density is included in the “core.” (a) $\epsilon=0$; (b) $\epsilon/\Delta=-0.5$.

Figures 8(a) and 8(b) illustrate the dynamics of $\sigma_z(t)$ versus the electron–phonon coupling, α . The parameters $\omega_c/\Delta=60$ and $\beta\Delta=10$ are the same as in Fig. 7. In Fig. 8(a) the electronic energy bias ϵ is zero, and in this parameter regime NIBA gives results in excellent agreement with the simulation. For $\alpha=0.5$, the expression in Eq. (3.8) is also in good agreement with both the NIBA and the simulation results. On the other hand, in Fig. 8(b) the electronic bias ϵ is nonzero, and here NIBA gives progressively worse results as α increases. In fact, it does not even conserve the total electronic population.

At very low temperature and/or high bath characteristic frequency ω_c , an approximation has been proposed previously for weak electron–phonon coupling cases.²⁸ Comparisons are made in Fig. 9 between this weak-coupling approximation (WCA) and the simulation. Overall, WCA gives quite good results for both zero and nonzero electronic energy bias ϵ (with a slight phase shift). NIBA, on the other hand, is very accurate for $\epsilon=0$, but much worse for a sizable ϵ .

IV. ELECTRONIC RESONANCE DECAY IN THE CONDENSED PHASE

One of the advantages of the method proposed in this paper is that many degrees of freedom are treated explicitly in the “core.” With respect to the numerical implementation, there is little difference between a subsystem and a bath. One can thus treat much larger subsystems than the two-state problem, with essentially no increase in the computational effort (if the bath properties remain unchanged). As an example, we consider the effect of a thermal bath on the electronic resonance decay.^{29,30}

A. Background of the problem

Short-lived electronic states that decay by electron emission into a continuum are an ubiquitous phenomenon in atomic and molecular physics. The corresponding resonances can be observed, for example, in photoionization and electron-scattering cross sections.³¹ In molecules the decay of electronic resonance states is significantly influenced by nuclear motion. Whereas the theory of resonant electron-molecule scattering appears to be well developed for small molecules (see, for example, Refs. 32, 33 for reviews), so far there have been relatively few attempts to provide a theoretical modeling of electronic resonance decay in larger polyatomic systems such as, for example, larger polyatomic molecules, molecular aggregates, or molecules adsorbed on surfaces.^{34–36,30} In such systems the electronic dynamics is coupled to a large number of vibrational modes and one of the interesting aspects is how this dissipative environment affects the decay dynamics of the resonance.

Here, we adopt a model which was proposed recently to study such processes.²⁹ Based on the projection-operator formalism,^{37,33} the model describes an isolated electronic resonance that can decay into a single electronic scattering channel and is coupled to a continuum of nuclear vibrations. In a basis of diabatic electronic states, consisting of a discrete state $|\phi_d\rangle$ (which represents the resonance) and a set of background scattering states $|\phi_k\rangle$, the Hamiltonian is written as

$$\hat{H} = \hat{H}_B + (\hat{H}_c + \epsilon_d)|\phi_d\rangle\langle\phi_d| + \sum_k |\phi_k\rangle\epsilon_k\langle\phi_k| + \sum_k (|\phi_d\rangle V_{dk}\langle\phi_k| + \text{H.c.}). \quad (4.1)$$

Here, $\epsilon_k = k^2/2$ denotes the asymptotic energy of a continuum electron and ϵ_d is the energy of the resonance state. H_B and H_c , as given in Eq. (3.2), represent the nuclear vibrational Hamiltonian and its coupling to the resonance state, respectively. As in the previous section, the nuclear vibrational continuum is represented by a Ohmic bath (with exponential cutoff), Eq. (3.4), which is discretized via Eqs. (3.6)–(3.7).

The discrete-continuum coupling element V_{dk} is specified by the energy-dependent decay width of the resonance,

$$\Gamma(E) = 2\pi \sum_k |V_{dk}|^2 \delta(E - \epsilon_k). \quad (4.2)$$

In the model considered here, this electronic width function is given by Wigner's threshold law³⁸ at low energies and a suitable cutoff function at high energies,

$$\Gamma_c(E) = A(E/B)^{l+(1/2)} \exp(-E/B), \quad (4.3)$$

where l denotes the lowest partial wave into which the resonance can decay according to symmetry selection rules.

The electronic continuum can be discretized by introducing a density of states $\Omega(E)$ satisfying

$$\int_0^{\epsilon_k} dE \Omega(E) = k, \quad k = 1, 2, \dots, \quad (4.4)$$

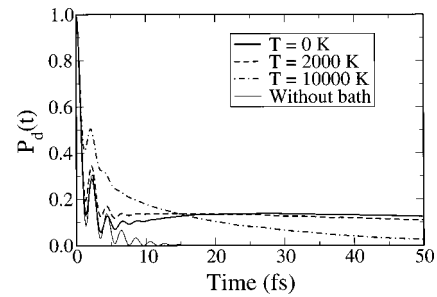


FIG. 10. Survival probability of the discrete resonance state, $P_d(t)$. The parameters are given in the text. The percentage of the bath modes (starting from the high-frequency end of the spectral density) in the “core” are 90%, 80%, and 40% for $T=0$ K, $T=2000$ K, and $T=10000$ K, respectively; and the number of bath modes are 50, 30, and 30, respectively. For comparison, $P_d(t)$ in the absence of the bath is displayed as the thin line.

and similar to Eq. (3.6), Eq. (4.3) is cast into the form of Eq. (4.2) via

$$|V_{dk}|^2 = \frac{1}{2\pi} \frac{\Gamma_c(\epsilon_k)}{\Omega(\epsilon_k)}. \quad (4.5)$$

For simplicity, we choose $\Omega(E)$ to be constant,

$$\Omega(E) = \frac{N_k}{E_{\max}}, \quad (4.6)$$

where N_k is the number of states that represent the electronic continuum, and E_{\max} is the energy for the highest electronic state, which is sufficiently large to ensure convergence.

The observable of interest, for studying the influence of the thermal bath on the decay of the electronic resonance, is the time-dependent survival probability of the resonance state,

$$P_d(t) = \frac{1}{Q_b} \text{tr}[e^{-\beta\hat{H}_b} |\phi_d\rangle\langle\phi_d| e^{i\hat{H}t} |\phi_d\rangle\langle\phi_d| e^{-i\hat{H}t}]. \quad (4.7)$$

Here, it is assumed that the electron is initially in the resonance state and the vibrational bath is in thermal equilibrium.

B. Results and discussion

With respect to the computational methodology described in this paper, the procedure for calculating the electronic resonance decay is nearly identical to that for the spin-boson problem. The only difference is that now we have N_k states instead of only two states. This makes negligible difference in both numerical implementation and the computational effort for similar (nuclear) bath properties.

Figure 10 displays the survival probability, $P_d(t)$, for the discrete resonance state. The parameters used here are³⁹ $A = 3.833$ eV, $B = 0.3$ eV, and $l = 2$ for the width function in Eq. (4.3); $\alpha = 16$ and $\omega_c = 0.2$ eV for the (nuclear) Ohmic bath in Eq. (3.4); and $\epsilon_d = 1.5$ eV for the discrete resonance state. A total of 50–100 discretized electronic states $|\phi_k\rangle$ with $E_{\max} = 3.5$ eV, and 30–50 nuclear bath modes, provide converged results within the timescale of simulation.

In the absence of coupling to the nuclear vibrations ($\alpha = 0$), the model does not possess bound states and, therefore, the resonance state decays completely to the electronic continuum. Due to the relatively high energy of the resonance

state ($\epsilon_d = 1.5$ eV), the time scale of the decay is rather fast. Furthermore, it is seen that the decay is nonmonotonic and exhibits pronounced coherent oscillations. As has been discussed in detail by Plöhn *et al.*, these oscillations are the result of the quantum beating of two resonance poles in this model. The coupling to the vibrational bath alters this decay dynamics qualitatively. The electronic energy present in the initial state can now be dissipated into the vibrational bath and is thus no longer available for the autodetachment process of the electron, thereby stabilizing the electron in the resonance state.⁴⁰ At zero temperature of the bath, this stabilization mechanism results in an incomplete decay, i.e., a finite population of the resonance state at longer times. This suggests that the electron–nuclear coupling induces bound states with finite overlap to the resonance state. As temperature increases, states with higher energies become more populated and eventually the resonance will completely decay to the electronic continuum. It is also seen that the kinetics of the resonance decay is changed when temperature increases; the initial decay becomes slower and the population dynamics undergoes a coherent to incoherent transition.

It should be pointed out that compared to molecular scattering processes, the electronic resonance decay problem considered here is relatively fast (with a typical time scale of tens of femtoseconds). The corresponding energy scale and coupling strength of the electronic resonance decay is, however, much larger. This makes the theoretical treatment more challenging for methods that are based on a nonlocal-time kernel such as the path-integral method of Ref. 29. For the present parameter regime, a stepsize of 0.1–0.3 fs and a kernel memory length of more than 50 time steps would be required for a path integral study,²⁹ which makes it unfeasible without making further approximations. This problem does not exist in the self-consistent hybrid method proposed in this paper because of its time-local nature. It is thus promising to apply the method to other complex processes with a large subsystem.

V. CONCLUDING REMARKS

In this paper, we have described a systematic way of achieving convergence in hybrid methods for complex molecular systems, the self-consistent hybrid method. In the first step, the overall system is partitioned into a “core” and a “reservoir,” based on any convenient but otherwise rather arbitrary initial guess. The dynamical hybrid calculation is then performed for this specific “core”–“reservoir” partition. The “core” is treated in a numerically exact fashion, using the basis set method in a multiconfiguration time-dependent Hartree (MCTDH) context. An appropriate approximate method, such as classical or semiclassical mechanics, or quantum perturbation theory, is used to treat the “reservoir.” Different from other previously applied hybrid methods, the partition of “core”–“reservoir” is not fixed *a priori*. Instead, it is cast into a self-consistent iterative procedure that in many ways resembles a usual variational calculation: the size of the “core” is gradually increased, to-

gether with other necessary variational parameters, to achieve numerical convergence. Therefore, the method is in principle numerically exact.

The efficiency and feasibility of the proposed self-consistent hybrid method are demonstrated by applying it to two problems in the condensed phase, the spin-boson problem and the electronic resonance decay in the presence of a nuclear bath. It is shown that for a broad parameter regime, the current method achieves numerical convergence with relatively few variational parameters. The resulting computations are easily achieved on a modern workstation.⁴² Considering the fact that the current method does not rely on integrating out any part of the overall system, it should be quite straightforward to apply the method to other complex problems with a large subsystem and/or anharmonic bath.

For the spin-boson problem, most of the transition behavior (rather than specific limits) shown in this paper cannot be predicted by any existing analytic theories. This is due to the ill time scale separation between electron and phonon motions, relatively large couplings, existing of a sizable energy bias between the two electronic states, or other important physical reasons. The correct description of such transitions are very important for the understanding of electron transfer mechanisms and building appropriate physical models that are crucial in interpreting various experiments for condensed phase systems. In those situations, the experimental information is often highly averaged. Preassuming a certain physical regime and subsequent application of approximate theories (applicable to that regime) often leave no room for other possible mechanisms that are lacking in the corresponding theories. The method proposed in this paper provides an unbiased way of investigating the true reaction mechanism, and also facilitates further development of approximate theories.

The self-consistent hybrid method provides both accurate and practical ways of dealing with various physical transitions. It is quite natural for this method to handle a transition from a “fast” bath (in general short memory length for the dynamical impact of the bath) to a “slow” bath (in general long time memory), as is shown in Figs. 3 and 5. On the other hand, it is also shown that the timescale of a bath mode is not the only criterion that determines its “quantum” or “classical” treatment. Convergence tests need to be carried out to ensure that the results are accurate, and sometimes other criteria are more efficient (e.g., Figs. 4 and 5). Neither is the method restricted to the mixed quantum-classical model. As demonstrated in the paper, a method that combines the MCTDH treatment for the “core” and a perturbative treatment for the “reservoir” is more efficient for very low temperatures. In this case the “core” contains the “slower” bath modes. A more thorough investigation of the spin-boson problem and comparisons with various approximate theories is given in the following paper.²²

For the problem of electronic resonance decay, it is shown that the electron–nuclear interactions effectively lower the energy level of the resonance state, thereby inducing localizations for electrons. Both the kinetics and the thermodynamic limit of the resonance decay are altered as the temperature of the nuclear bath changes. A coherent–

incoherent transition occurs as the temperature increases, with the resulting initial decay becoming slower. This problem contains rich physics and deserves further theoretical investigation.

In the current self-consistent hybrid method, a “good” initial guess for the “core”–“reservoir” can accelerate the iterative process, but is somehow difficult to choose without some knowledge of the specific problem. This is similar to other variational calculations, where certain approximate theories may help in picking such an initial guess. In the mixed quantum-classical calculations, we start by treating only the electronic states in the “core,” i.e., using the classical Ehrenfest model, with only the electronic degree of freedom treated quantum mechanically, as our initial guess. Usually more than 10 iterations are needed before reaching final convergence. A better initial guess, after investigating broad parameter regimes, is empirically found for the spin-boson problem that bath modes with $\omega > (0.5 - 1)k_B T$ usually need to be treated in the “core.”

There are other techniques that can further improve the numerical efficiency of the current method. For example, one can put some important and strongly coupled collective degrees of freedom, the *reaction coordinates*, into the “core” for rigorous treatment, so that most of the remaining degrees of freedom can be treated more approximately. There is certainly much to be done to explore such methods that are applicable to even more complex systems. The current method provides both benchmark results and essential ingredients for such development.

ACKNOWLEDGMENTS

This work was supported by the Director, Office of Science, Office of Basic Energy Sciences, Chemical Sciences Division of the U.S. Department of Energy under Contract No. DE-AC03-76SF00098, and by National Science Foundation Grant No. CHE 97-32758. One of the authors (M.T.) gratefully acknowledges a Feodor-Lynen fellowship of the Alexander von Humboldt Foundation and thanks W. Domcke for numerous helpful discussions.

¹N. F. Mott, Proc. Cambridge Philos. Soc. **27**, 553 (1931).

²J. B. Delos and W. R. Thorson, Phys. Rev. A **6**, 720 (1972).

³(a) G. D. Billing, Chem. Phys. Lett. **30**, 391 (1975); (b) J. Chem. Phys. **99**, 5849 (1993).

⁴(a) R. B. Gerber, V. Buch, and M. A. Ratner, J. Chem. Phys. **77**, 3022 (1982); (b) V. Buch, R. B. Gerber, and M. A. Ratner, Chem. Phys. Lett. **101**, 44 (1983).

⁵D. A. Micha, J. Chem. Phys. **78**, 7138 (1983).

⁶R. Graham and M. Höhnerbach, Z. Phys. B: Condens. Matter **57**, 233 (1984).

⁷(a) R. K. Preston and J. C. Tully, J. Chem. Phys. **54**, 4297 (1971); (b) **55**, 562 (1971); (c) J. C. Tully, *ibid.* **93**, 1061 (1990).

⁸M. F. Herman, J. Chem. Phys. **76**, 2949 (1982).

⁹F. J. Webster, P. J. Rossky, and R. A. Friesner, Comput. Phys. Commun. **63**, 494 (1991).

¹⁰S. Chapman, Adv. Chem. Phys. **82**, 423 (1992).

¹¹For reviews see W. H. Miller, Faraday Discuss. **110**, 1 (1998).

¹²A. A. Golosov, R. A. Friesner, and P. Pechukas, J. Chem. Phys. **112**, 2095 (2000).

¹³R. P. Feynman and A. R. Vernon, Ann. Phys. (N.Y.) **24**, 118 (1963).

¹⁴For reviews see M. H. Beck, A. Jackle, G. A. Worth, and H.-D. Meyer, Phys. Rep. **324**, 1 (2000).

¹⁵(a) H.-D. Meyer, U. Manthe, and L. S. Cederbaum, Chem. Phys. Lett. **165**, 73 (1990); (b) U. Manthe, H.-D. Meyer, and L. S. Cederbaum, J. Chem. Phys. **97**, 3199 (1992).

¹⁶(a) G. Worth, H.-D. Meyer, and L. S. Cederbaum, J. Chem. Phys. **109**, 3518 (1998); (b) A. Raab, G. A. Worth, H.-D. Meyer, and L. S. Cederbaum, J. Chem. Phys. **110**, 936 (1999).

¹⁷I. Burghardt, H.-D. Meyer, and L. S. Cederbaum, J. Chem. Phys. **111**, 2927 (1999).

¹⁸H. Wang, J. Chem. Phys. **113**, 9948 (2000).

¹⁹This seems to be a ubiquitous problem in a basis set calculation; the most difficult regime for which to converge is the high temperature/low frequency regime, where many basis functions (grid points) are needed to describe an often trivial decoherence limit (classical limit) that is easily captured by classical mechanics.

²⁰(a) H. Wang, X. Sun, and W. H. Miller, J. Chem. Phys. **108**, 9726 (1998); (b) X. Sun, H. Wang, and W. H. Miller, *ibid.* **109**, 4190 (1998); (c) **109**, 7064 (1998); (d) H. Wang, X. Song, D. Chandler, and W. H. Miller, *ibid.* **110**, 4828 (1999).

²¹Z. Bačić and J. C. Light, J. Chem. Phys. **85**, 4594 (1986).

²²M. Thoss, H. Wang, and W. H. Miller, J. Chem. Phys. **115**, 2991 (2001), following paper.

²³A. J. Leggett, S. Chakravarty, A. T. Dorsey, M. P. Fisher, A. Garg, and W. Zwerger, Rev. Mod. Phys. **59**, 1 (1987).

²⁴U. Weiss, *Quantum Dissipative Systems* (World Scientific, Singapore, 1993).

²⁵N. Makri and D. E. Makarov, J. Chem. Phys. **102**, 4600 (1994).

²⁶D. E. Makarov and N. Makri, Chem. Phys. Lett. **221**, 482 (1994).

²⁷G. Stock, J. Chem. Phys. **103**, 1561 (1995).

²⁸M. Grifoni, E. Paladino, and U. Weiss, Eur. Phys. J. B **10**, 719 (1999).

²⁹H. Plöhn, M. Thoss, M. Winterstetter, and W. Domcke, Phys. Rev. A **58**, 1152 (1998).

³⁰M. Thoss and W. Domcke, J. Chem. Phys. **109**, 6577 (1998).

³¹G. J. Schulz, Rev. Mod. Phys. **45**, 378 (1973); **45**, 423 (1973).

³²N. F. Lane, Rev. Mod. Phys. **52**, 29 (1980).

³³W. Domcke, Phys. Rep. **208**, 97 (1991).

³⁴J. P. Gauyacq and A. Herzenberg, J. Phys. B **17**, 1155 (1984); **23**, 3041 (1990).

³⁵M. Winterstetter and W. Domcke, Phys. Rev. A **47**, 2838 (1993); **48**, 4272 (1993).

³⁶H. Tachikawa, J. Phys. Chem. **101**, 7454 (1997).

³⁷H. Feshbach, Ann. Phys. (N.Y.) **19**, 287 (1962).

³⁸E. P. Wigner, Phys. Rev. **73**, 1002 (1948).

³⁹These parameters correspond to model III in Ref. 29. It should be noted that the parameter α for model II and II were misprinted in Ref. 29. The results shown there are for an eight times larger value of α . Also, note that due to the different definitions of the spectral densities there is an additional factor of 4 between the parameter α used here and the α in Ref. 29.

⁴⁰This mechanism is similar to the “polaron” problem, where the electron is dressed by a phonon cloud which has the tendency to localize the electron, Ref. 41.

⁴¹(a) T. Holstein, Ann. Phys. (N.Y.) **8**, 325 (1959); **8**, 343 (1959); (b) D. Emin, Adv. Chem. Phys. **24**, 305 (1975).

⁴²For all the examples considered in this paper, the CPU is between one and ten hours with a converged statistical sampling size of $10^2 - 10^4$.